3.
Carbon Dioxide
(CO_2)

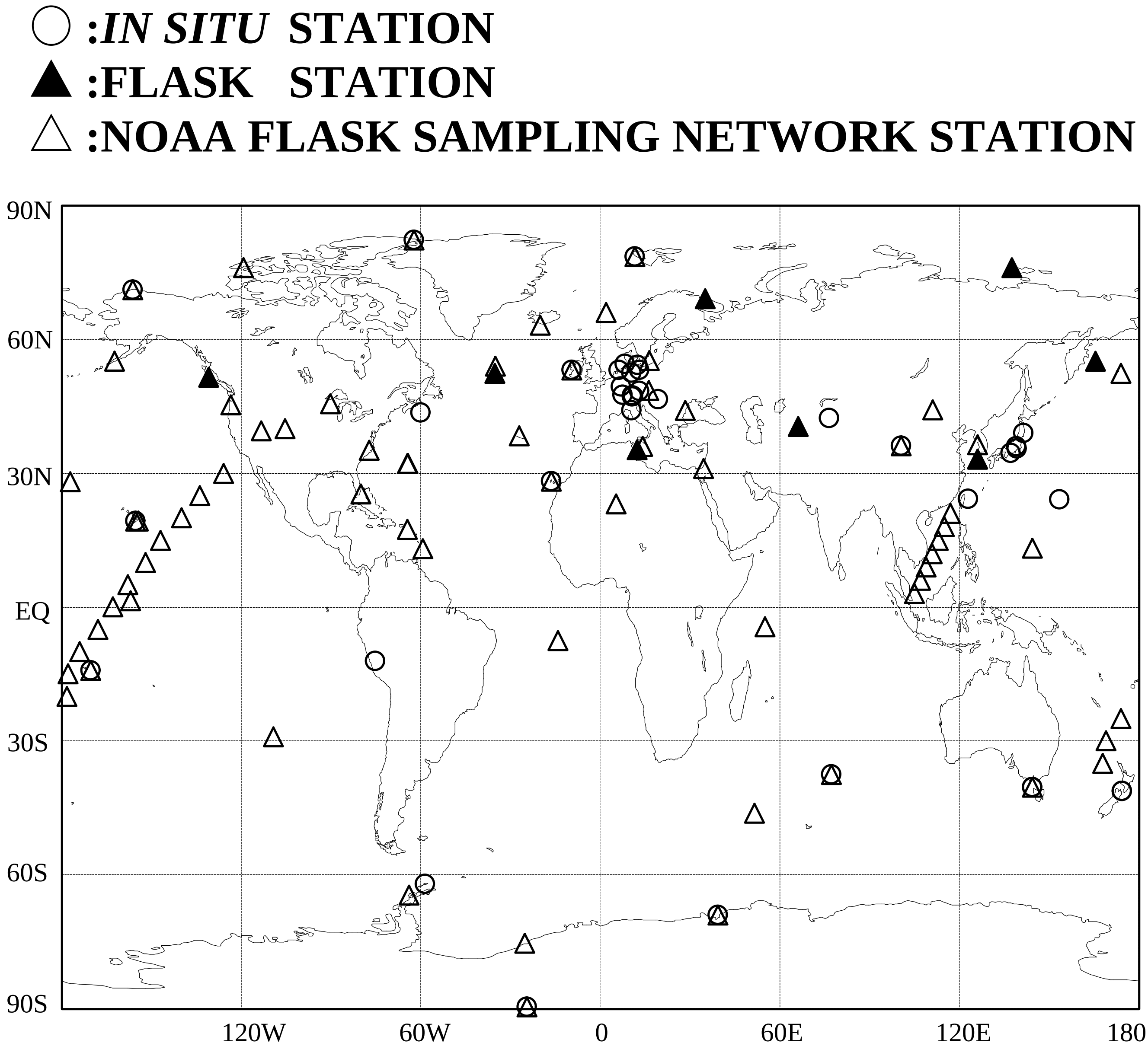

3. Carbon Dioxide (CO_2)

Carbon dioxide (CO_2) is a significant greenhouse gas that is the largest contributor to global warming. Before the 18th century (pre-industrial times) the concentration of carbon dioxide in the atmosphere was about 280 ppm based on ice core studies, while in 1997 the concentration was about 364 ppm at Mauna Loa (NOAA/CMDL, 1998). More than half of the direct radiative forcing from the increase in long-lived greenhouse gases is attributed to that of carbon dioxide (IPCC, 1996).

CO_2 is emitted by and absorbed on the Earth's surface in different ways, including respiration and photosynthesis by the terrestrial biosphere, exchange with oceans, and human activity such as fossil fuel combustion and land-use changes. Since the 18th century, increasingly emitted anthropogenic CO_2 has been distributed in the atmosphere, oceans, and terrestrial biosphere, which serve as reservoirs of CO_2 in the global carbon cycle. About half of this amount remains in the atmosphere and the rest is removed by sinks, including forest regrowth and ocean uptake. Carbon isotope studies have successfully showed the significant importance of the terrestrial biosphere and oceans as sources and sinks (Francey *et al.*, 1995; Keeling *et al.*, 1995; and Nakazawa *et al.*, 1993,1997a), and there is increasing recognition of the importance of carbon isotope data.

Large amounts of CO_2 in reservoirs are exchanged among these areas, and the global carbon cycle is coupled with the climate system on seasonal, interannual, and decadal time-scales. Understanding of the global carbon cycle is essential to produce an accurate estimate of future CO_2 concentrations in the atmosphere.

At the head of this chapter, operational observation sites on the ground and shipboard that submitted CO_2 concentration data to the WDCGG until June 1999 have been shown on a map. They include *in situ* stations measuring continuously and flask-sampling stations such as the ones in the NOAA/CMDL network. In addition to such fixed stations, mobile stations on ships and aircraft and other stations measuring on a campaign (event data) also report their data to the WDCGG (Appendix: LIST OF OBSERVING STATIONS).

3.1 Analysis of global, hemispheric, and zonal mean concentrations

Global, hemispheric, and zonal mean concentrations were derived from data calibrated on the WMO mole fraction scale. For the analysis, long-term data with a record of more than 3 years was only used to calculate zonal, hemispheric, and global averages. The data came from stations that were not affected by the local environment and located not only in oceanic but also in continental regions.

Figure 3.1 shows monthly mean concentrations and their deseasonalized long-term trend from 1983 to 1997 for the globe and for both hemispheres. Long-term increases in both hemispheres and seasonal variation in the Northern Hemisphere are clearly seen. The annually averaged concentration is 363 ppm in 1997 for the globe. Figure 3.2 shows growth rates for the same areas as in Figure 3.1. The average growth rate over this period (1983–1997) is 1.5 ppm/year for the globe. In terms of the growth rate for the globe, the maximum is 2.7 ppm/year in the spring of 1987 and the minimum is 0.6 ppm/year in the autumn of 1992. High growth rates of above 2 ppm/year are seen in 1983,1987/1988, and 1994/1995.

Figure 3.3 shows monthly mean concentrations and their deseasonalized long-term trend from 1983 to 1997 for each 30-degree latitudinal zone. Deseasonalized concentrations are the highest in northern high or mid-latitudes, suggesting regions with a strong net source in these latitudes.

Figure 3.4 shows analytical results for the deseasonalized long-term trend, growth rates, and annual amplitudes of seasonal cycles. Variations of growth rates are seen over time. Growth rates are high in 1983, 1987/1988, and 1994/1995, and are low in 1984/1985, 1989/1990, 1992/1993 with a negative value in the northern high latitudes, and 1996. Variability in the growth rate is comparatively large in northern high and mid-latitudes and small in southern latitudes, suggesting significantly varying activity of sources and sinks in northern high and mid-latitudes.

Changes in growth rate are also known to be associated with El Niño-Southern Oscillation (ENSO). El Niño events occurred in 1982/1983, 1986-1988, 1991/1992, 1993, and 1997/1998. Correspondingly, growth rates were high in 1983, 1987/1988, and 1994/1995, but low in 1992. Carbon isotope (^{13}C) studies are used to clarify how terrestrial and oceanic sinks contribute to such variations (Francey *et al.*, 1995; Ciais *et al.*, 1995; and Keeling *et al.*, 1995). They suggest that changes in the growth rate during El Niño events may reflect two opposing effects: reduced uptake by the terrestrial biosphere and increased uptake by oceans. The former effect is brought about by high global temperature through activated respiration of plants and decomposition of organic matter in soil. Sparse precipitation particularly in the tropics also enhances this effect by suppressing plant photosynthesis. The latter is caused by weak upwelling CO_2-rich water in the eastern equatorial Pacific. In usual cases, the former effect surpasses the latter, resulting in increased growth rates (Dettinger *et al.*, 1998). However, the El Niño event in 1991/1992 was an exception. The lower temperature after the eruption of Mt. Pinatubo reduced emission from the northern terrestrial biosphere and increased uptake to the global oceans (Rayner *et al.*, 1999).

An anomalously strong El Niño event occurred in 1997/1998. The climate system involving the atmosphere, oceans, land, terrestrial biosphere, and so on largely deviated from normal conditions (JMA, 1999; WMO, 1999b). Anomalously scarce precipitation brought about frequent droughts and forest fires in Southeast Asia in 1997/1998, and the global mean temperature was the highest recorded in 1998. Such extreme climate conditions perturbed the global carbon cycle, and accelerated the increase of CO_2 concentrations in the atmosphere. The highest annual increase in atmospheric CO_2 concentration was observed at Mauna Loa (Bell *et al.*, 1999) and Ryori, Japan (Watanabe *et al.*, 1999) in 1998.

Figure 3.5 draws average seasonal cycles for each 30-degree latitudinal zone. Seasonal variation in CO_2 concentration is basically induced by absorption and emission in the terrestrial biosphere, which is typically absorption by photosynthesis and emission by respiration in vegetation and decomposition by microbes in soil (e.g. Nakazawa *et al.*, 1997b). Ocean uptake (Ramonet *et al.*, 1996) and biomass burning (Wittenberg *et al.*, 1998) are also thought to influence the seasonal variation.

Amplitudes of seasonal cycles are clearly large in northern high and mid-latitudes and small in the Southern Hemisphere. The northern seasonal cycle reflects seasonal variation in absorption/emission in the biosphere there. The small amplitudes in the Southern Hemisphere are attributed to small amounts of absolute emission/absorption by the terrestrial biosphere and adverse contributions of oceans and biomass burning. In southern low latitudes, an annual cycle cannot be seen clearly but a semiannual cycle can. This is probably due to two opposing factors, i.e., the direct influence of sources and sinks in the Southern Hemisphere and diffusion of out-of-phase seasonal variation from the Northern Hemisphere.

Months of maximum concentration in the seasonal cycle appear in early spring in northern mid-latitudes, and one or two months later in northern high and low latitudes. Months of minimum concentration appear in August in northern high and mid-latitudes and in September in northern low latitudes. The later peak months in low latitudes arise from delayed propagation of the variation from higher latitudes (Tanaka *et al*., 1987).

Months of maximum concentration in the seasonal cycle appear in austral early spring in southern high and mid-latitudes, and minimum concentration in austral early autumn. In southern high and mid-latitudes, the seasonal cycle partly reflects oceanic variations.

More detailed discussions and figures about seasonal variations are referred to in the previous issue of *Data Summary* (WMO, 1998).

3.2 Analysis for individual stations

Time-series analysis was also used for stations representing global or regional situations: Point Barrow (Alaska, U.S.A.), Mauna Loa (Hawaii, U.S.A.), Baring Head (New Zealand), the South Pole (Antarctica), Schauinsland (Germany), and Ryori (Japan), which were selected after taking into account the data record length and geographical distribution. Figure 3.6 shows a time series of monthly mean concentrations, deseasonalized long-term trends, growth rates, and amplitudes of seasonal cycle and months with maximum and minimum values for each year for each of the stations mentioned. Figure 3.7 draws average seasonal cycles for each station.

At Ryori and Baring Head, the growth rate was the highest in 1997/1998 since the beginning of observation. The highest annual increase was also observed at Mauna Loa (Bell *et al*., 1999). These extremely high growth rates observed worldwide were probably caused by the anomalously strong El Niño event in 1997/1998. The lower temperature influenced all of the stations after the eruption of Mt. Pinatubo, but the growth rates decreased with different timing. In the northern high and mid-latitude stations, i.e., Point Barrow, Schauinsland, and Ryori, the lowest growth rates were recorded from the end of 1991 to the beginning of 1992. In the northern low-latitude and the southern stations, i.e., Mauna Loa, Baring Head, and the South Pole, however, the rates were seen from the end of 1992 to the beginning of 1993.

The amplitude of the seasonal cycle is considerably large at Ryori, but activities in the terrestrial biosphere make the amplitudes much larger at Point Barrow and Schauinsland.